Hindawi
Wireless Communications and Mobile Computing
Volume 2021, Article ID 8847008, 11 pages
https://doi.org/10.1155/2021/8847008

Research Article

The Design of a Class of Nonlinear Networked System

Biao Wang, Xing Zhao, Changbo Li, Ji Ke, Yude Qin, Hao Wu, and Hang Yang

College of Electronic & Control Engineering Chang'an University, Xi'an, China

Correspondence should be addressed to Biao Wang; wangbiao@chd.edu.cn

Received 15 September 2020; Revised 29 January 2021; Accepted 18 February 2021; Published 11 March 2021

Academic Editor: Changqing Wang

A class of nonlinear networked systems with external interference is designed in this paper. Currently, we have witnessed that networked control technology has played a key role in the Internet of Things (IoT). However, the amount of big data in the Internet of Things will cause network congestion in the data transmission of the network control system. In order to solve this problem, event-driven control scheme can effectively save the network resources of the network control system. But when there is interference in the system, the conventional constant threshold parameter is difficult to achieve the expected energy-saving effect. In order to solve this challenge, this paper proposes a design with a continuously variable threshold. After each trigger to transmit data, the threshold gets changed accordingly, and the sliding mode approach rate is changed simultaneously. Compared with the constant threshold event drive, the number of transmissions in this design can be greatly reduced, while sliding mode jitter is suppressed. The simulation results show that the scheme can achieve higher resource utilization efficiency and better robustness.

1. Introduction

In recent years, we have witnessed the rapid development of the Internet of Things (IoT). By 2020, the surge in mobile devices is expected to exceed 50 billion. NCS research plays a key role in this field. At present, networked-control systems (NCSs), including multiloop NCSs, are extensively used. Their systems have the advantages of high reliability, high system flexibility, and low installation and maintenance costs [1–6]. Network control systems are used in many fields, such as mobile sensor networks [7], intelligent transportation systems [8], remote network control technologies [9], and theoretical results in [2, 3, 10] and other applications. In general, for the control of IoT, the collection and processing of data are very important. Note that with the emergence of IoT, the captured data will increase significantly. In the network control system (NCS), when the network is congested, phenomena such as jitter, packet loss, and transmission delay are particularly prone to occur [11–13], leading to poor performance of the network control system. Therefore, it is urgent to design a reasonable control scheme to reduce data transmission on the network. This solution should ensure that the network control system still has satisfactory performance even in the presence of uncertainty and delayed transmission.

In the past few decades, scientific literature has proposed several control schemes to save communication network transmission resources [14–16]. Event driving (ED) is one of the widely recognized and effective methods [17–24]. In traditional time-driven control schemes, data is transmitted periodically. Unlike the traditional implementation of time-driven control, the ED control scheme allows communication between the controlled object and the controller (feedback path) and between the controller and the actuator (direct path) only when certain trigger conditions are met. Therefore, the ED control method can significantly reduce data transmissions and avoid network congestion and its possible unavailability. In [25], the authors propose a decentralized event-driven implementation of a centralized nonlinear controller on a sensor-actuator network. In [26], Wang and Lemmon assumed that the control system was composed of weakly coupled subsystems and proposed a

distributed event-driven control method. In [27], the authors developed an event-driven transmission strategy based on state estimation. Designing event-driven algorithms based on changes in the Lyapunov function and selection of input variables to be updated is given in [28]. The threshold value of the event driving condition may greatly affect the execution of the control task. In recent years, a common design method for the feedback control gain of the system and the parameters of the event driving condition has been studied, such as [29–32] and references in the text.

The aforementioned event driving scheme (EDS) has a common feature that the threshold value of the event driving condition is known in advance. Since the threshold value is a preset constant, it is difficult to adapt to changes in the system; that is, the designed event driving parameters cannot adapt to external disturbances. To overcome this shortcoming, event trigger parameters need to be optimized online to achieve adaptation to external disturbances. But so far, there are few researches on the variable threshold under the event-driven condition of nonlinear systems in the public literature. Increasing the anti-interference ability of the event-driven system is a factor that must be considered in the design of high-performance event-driven control systems. Increasing the anti-interference ability of the event-driven system is a factor that must be considered in the design of high-performance event-driven control systems. Sliding mode control (SMC) is a well-known robust control method, which is especially suitable for models subject to modeling uncertainty and external interference control system [33, 34]. Due to its robustness, sliding mode control is also an effective control method based on the arrival law, which greatly improved the fast convergence of the sliding mode surface under the excessive strategy for networked control systems [35, 36]. Asifa Yesmin et al. proposed an event-driven sliding mode control jitter and gave designers greater freedom to design parameters to achieve: the expected steady state in the absence of disturbance uncertainty [37]. An event-driven sliding mode controller with a fuzzy variable threshold is designed for a nonlinear continuous time-varying MIMO system. The fuzzy control is used to variablely adjust the event trigger condition threshold of the nonlinear system to make the system more flexible.

The main contributions of this paper include the following: (1) designing event-driven control with fuzzy control for nonlinear continuous time-varying MIMO systems based on sliding mode control; (2) designing a novel variable event driving condition for nonlinear systems, in order to promote system stability and speed, while reducing network data transmission; and (3) the formula which is used to prove and simulate the closed-loop stability of the system.

The content of this article is arranged as follows: the second part introduces the system description and continuous-time sliding mode control, the third part introduces the event-driven sliding mode controller design, and then the fourth part introduces the fuzzy control and event driven control (EDC) variable design. The numerical example simulation in Section 5 validates the analysis results. Finally, conclusions are drawn in Section 6.

2. System Description and Sliding Mode Control

2.1. System Description. First, we consider a MIMO nonlinear system, as shown below:

$$\dot{\mathbf{x}} = \mathbf{f}(\mathbf{x}) + \mathbf{B}u + \mathbf{B}d. \tag{1}$$

Here, $\mathbf{x} = [x_1, x_2] \in R^{2n}$, $\mathbf{f}(\mathbf{x}) = [f_1(x_1), f_2(x_1, x_2)]$, $\mathrm{B} \in R^{2n}$, x_1, and $x_2 \in R^n$ represent the system's state variables. $\mathrm{u} \in R^n$ is the control input vector of the system, and d is the external disturbance affecting the system. It is assumed that the disturbance is bounded, i.e., $\sup_{t\geq 0}|d(t)| \leq d_0 < \infty$, and it satisfies the matching condition with respect to the control input.

For the nonlinear functions $f_1(\bullet)$ and $f_2(\bullet, \bullet)$, we make the following assumptions.

Assumption 1. The function $f_1(x_1)$ has a unique equilibrium point without loss of generality, and we assume $f_1(0)=0$. In addition, the system can be represented by both linear and nonlinear terms, such as $f_1(x_1)=A_1x_1 + \gamma(x_1)$, A_1 is a linearized system at the equilibrium point, and $\gamma(x_1)$ is the nonlinear components of higher-order terms.

Assumption 2. In the compact domain $D \in R^{2n}$, the functions $f_1(\bullet)$ and $f_2(\bullet, \bullet)$ are Lipschitz functions. For any vector z_1, z_2 in D, which are satisfied, $\|f(z_1) - f(z_2)\| \leq L\|z_1 - z_2\|$.

$$\begin{aligned} ||f(\xi_1) - f(\xi_2)|| &= ||f(z_1, y_1) - f(z_2, y_2)|| \\ &\leq \|f_1(z_1) - f_1(z_2)\| + ||B_1(y_1 - y_2)|| \\ &\quad + |f_2(z_1, y_1) - f_2(z_2, y_2)| \leq L_1||z_1 - z_2|| \\ &\quad + \|B_1\||y_1 - y_2| + |f_2(z_1, y_1) - f_2(z_2, y_2)| \\ &= (L_1 + L_2)||z_1 - z_2|| + (||B_1|| + L_2)|y_1 - y_2| \\ &\leq (L_1 + L_2)\|\xi_1 - \xi_2\| + (||B_1|| + L_2)\|\xi_1 - \xi_2\| \\ &= (L_1 + 2L_2 + ||B_1||)\|\xi_1 - \xi_2| = L\|\xi_1 - \xi_2\| \end{aligned} \tag{2}$$

2.2. Design of Sliding Mode Controller. Considering the nonlinear MIMO system given above, here, we choose $s = \mathbf{c}^T\mathbf{x}$ as the sliding mode surface of the system, where $\mathbf{c} \in R^n$.

$$S = \left\{\mathbf{x} \in R^n : s = \mathbf{c}^T\mathbf{x} = 0\right\}, \tag{3}$$

where $\boldsymbol{c} = [c_1^T \bullet 1]^T$ and $c_1 \in R^{n-1}$, $\boldsymbol{x} = [x_1^T \bullet x_2]^T$. Differentiating $s = \boldsymbol{c}^T\boldsymbol{x}$ with respect to time, we obtain:

$$\begin{aligned} \dot{s} = c_1^T\dot{x}_1 + \dot{x}_2 &= c_1^T f_1(x_1) + c_1^T\mathbf{B}_1x_2 + f_2(x_1, x_2) \\ &\quad + \mathbf{B}_2u + \mathbf{B}_2d = c^T f(\mathbf{x}) + \mathbf{B}_2u + \mathbf{B}_2d. \end{aligned} \tag{4}$$

The SMC design must ensure that the system trajectory converges to the sliding manifold, so the system trajectory must be converged to the equilibrium point within a limited time. Here, we design the control rate u as shown below:

$$u = -\mathbf{B}_2^{-1}\left(c^T f(\mathbf{x}) + K \operatorname{sign} s\right). \tag{5}$$

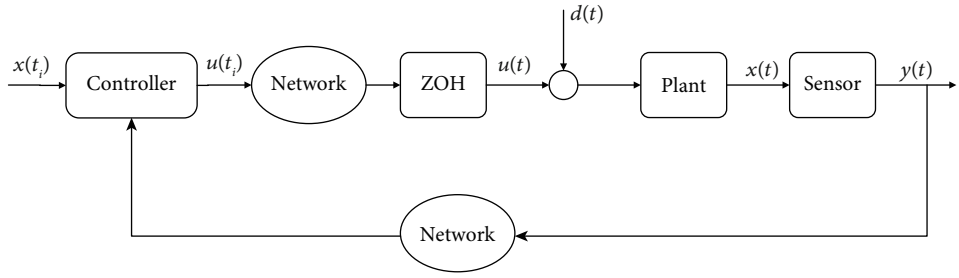

Figure 1: ED-SMC network controller architecture.

In the above formula, the gain K is a bounded constant and satisfies $K > |\mathbf{B}_2|d_0$. Therefore, the reaching law of sliding mode can be expressed as

$$\dot{s} = -K \text{ sign } s + \mathbf{B}_2 u. \tag{6}$$

The design of the control law and the approach law of the sliding mode controller ensures that the system can reach an equilibrium state in a finite lime. This chapter mainly analyzes the implementation of the SMC in the normal state. In the following content, we mainly analyze the implementation of the SMC in the event-driven state and consider the threshold of the ED-SMC trigger condition to design a variable event-driven sliding mode controller that meets the control performance.

3. Event-Driven Sliding Mode Controller

At present, there are few studies on SMC discretization of nonlinear systems. Similar to a linear system, the implementation of a discrete SMC, in this case, will never produce an accurate sliding mode, which is $s = 0$. Therefore, for discrete cases, the sliding trajectory does not remain on the switching manifold but remains near the sliding surface. In the SMC periodic operation, the final limit depends on the sampling interval and the perturbation limit. As the sampling interval decreases, the system performance improves accordingly. On the other hand, the steady-state boundary is designed in advance for the implementation of event driving, so performance can be improved as desired.

In order to make the system reach the tracking target in a limited time and keep the tracking error within a certain limit, the following content mainly studies the sliding mode controller with an event trigger. For example, in the LTI system, the trajectory of a nonlinear system simply depends on the design of some parameters to keep it within a certain range. In the following, the standard definition of the sliding mode of nonlinear systems based on the event-driven mechanism is given, and an event-driven sliding mode controller that meets the performance indicators is designed.

3.1. Design of Event-Driven Sliding Mode Controller. For the LTI system, the trajectory of the system stays constant within a certain range has nothing to do with the sampling interval. We can use the event trigger strategy to make the sliding mode motion reach any ideal stable state. This control will be kept constant until the next trigger Time is coming. $\{t_i\}_{i-=0}^{\infty}$ is a series of driving moments for control updates. Here, $T_i = t_{i+1} - t_i$ is used to represent the time of internal events. In Figure 1, the role of the zero-order retainer is to keep the data at the time $t \in [t_i, t_{i+1})$, so once the control is updated, the controller will continue to the next time t_{i+1}, before that the control signal has been $u(t) = u(t_i)$. We define $\mathbf{e}(t) = \mathbf{x}(t_i) - \mathbf{x}(t)$ as the systematic error. The error e here plays a very important role in the implementation of event-driven control. The main performance is by constantly observing the change of e until it reaches a preset threshold and then using this to determine the next time t_{i+1}. The event trigger mechanism has the advantage of reducing network signal transmission, saving network resources, and saving energy consumption. Moreover, this strategy will determine the state evolution and disturbance steady-state boundary in advance no matter what.

The design of the event-driven sliding mode controller here should also be divided into two steps: First, we need to design this sliding variable $s(t) = \mathbf{cx}(t) = x_1(t) + x_2(t)$, $\boldsymbol{c} = [1\ 1] \otimes I_{nn} \in R^{2n}$, and define this sliding mode surface as follows:

$$S = \{\mathbf{x} \in R^n : \|s\| = \|\mathbf{cx}\| \le u\}. \tag{7}$$

In the above formula, $u > 0$, because S here means "the practical sliding surface" [21].

In the second step, in order to enable the system trajectory to reach the sliding die surface, we should also design appropriate driving rules and control laws. The design of driving rules and control laws is given below.

Since the control signal remains constant in the time interval (t_i, t_{i+1}) between two consecutive driving moments, the control law can be written as follows:

$$u(t) = -\mathbf{B}_2{}^{-1}\left(\mathbf{c}^T f(\mathrm{x}(t_i)) + K \text{ sign } s(t_i)\right). \tag{8}$$

The purpose here is to design the switching gain so that the stability of the system trajectory remains for a limited time.

Theorem 3. *Considering the above nonlinear system and the given control law, let $\alpha > 0$, and give the following trigger conditions:*

$$L||\mathbf{c}||||e(t)|| < \alpha. \tag{9}$$

All time $t > 0$ here, if the gain K is selected as follows, the

actual sliding mode will appear in the system.

$$K > |\mathbf{B}_2|d_0 + \alpha. \tag{10}$$

Proof. Consider the Lyapunov function $V = 1/2S^2$. Differentiating V with respect to time $t \in [t_i, t_{i+1})$, we obtain the following:

$$\dot{V}(s) = s\dot{s} = s\left(\mathbf{c}^T f(\mathbf{x}) + \mathbf{B}_2 u + \mathbf{B}_2 d\right). \tag{11}$$

Taking the control law u (8) into the above formula, we get the following:

$$\begin{aligned}\dot{V}(s(t)) &= s(t)\left(\mathbf{c}^T f(\mathbf{x}(t))\mathbf{c}^T f(\mathbf{x}(t)) - c^T f(\mathbf{x}(t_i))\right.\\ &\quad - K \text{ sign } s(t_i) + \mathbf{B}_2 d \le -s(t)K \text{ sign } s(t_i)\\ &\quad + |s(t)|\left|\left|\mathbf{c}^T f(\mathbf{x}(t)) - \mathbf{c}^T f(\mathbf{x}(t_i))\right|\right| + |s(t)||\mathbf{B}_2|d_0\\ &\le -s(t)K \text{ sign } s(t_i) + |s(t)|||\mathbf{c}||||f(\mathbf{x}(t)) - f(\mathbf{x}(t_i))||\\ &\quad + |s(t)||\mathbf{B}_2|d_0 \le -s(t)K \text{ sign } s(t_i)\\ &\quad + |s(t)|L||\mathbf{c}||||\mathbf{x}(t) - \mathbf{x}(t_i)|| + |s(t)||\mathbf{B}_2|d_0.\end{aligned} \tag{12}$$

Until this trajectory reaches the sliding surface, the sign of the sliding variable will not change, and sign $s(t_i)$ = sign $s(t)$; we can write it as $-K \mid s(t) \mid$ And by taking equations (9) and (10) into (12), we can get

$$\begin{aligned}\dot{V}(s(t)) &\le -\mid s(t)|K + |s(t)|\alpha + |s(t)||\mathbf{B}_2|\mathrm{d}_0\\ &= -|s(t)|(K - \alpha - |\mathbf{B}_2|d_0) = -\eta|s(t)|.\end{aligned} \tag{13}$$

For some $\eta > 0$. This shows that in the time interval $[t_i, t_{i+1})$, for some $i \in Z \ge 0$, the trajectory is moving toward the sliding surface. For as long as sign $s(t_i)$ = sign $s(t)$, the interval is subsequently triggered. In the end, the tracking trajectory reaches the sliding surface in a limited time. However, there is no guarantee that the trajectory will still move on the sliding surface because no control signal is applied. Therefore, the trajectory passes through it after reaching the sliding surface. However, since relationship (9) holds, it will not be borderless, as shown below. We can get the maximum differential of the sliding trajectory at any time interval $[t_i, t_{i+1})$. It can be expressed by the following formula:

$$|s(t_i) - s(t)| = \left|\mathbf{c}^T x(t_i) - \mathbf{c}^T x(t)\right| \le ||\mathbf{c}||||\mathbf{e}(t)|| < \frac{\alpha}{L}. \tag{14}$$

If the trigger occurs when the trajectory just reaches the sliding mode surface, the maximum value of the actual sliding mode band can be obtained, so this boundary can be given as follows:

$$\Omega = \left\{\mathbf{x} \in \mathrm{D} : |\mathrm{s}| = |\mathbf{c}^T\mathbf{x}| < \frac{\alpha}{L}\right\}. \tag{15}$$

This indicates that the system trajectory ends up in the Ω region. Therefore, the certification is complete.

The above results have some similarities with linear systems. The first one is the relationship (9), which is essential for the existence of actual sliding modes in nonlinear systems. The Lipschitz constant that appears here corresponds to the induced norm of the system matrix of the LTI system. Another similarity is that the actual sliding mode band is obtained from a similar relationship (9) obtained with the LTI system.

3.2. System Stability Analysis. For the trigger conditions and control laws given above, we should analyze the closed-loop stability of the system. Redefine the sliding variable here, as shown below:

$$x_2(t) = -x_1(t) + s(t). \tag{16}$$

For the above algebraic dynamic equation, it can be proved that if $x_1(t)$ is bounded, then $x_2(t)$ must also be bounded. Below, we will prove the closed-loop stability of the system.

Here, $V_1 = (1/2){x_1}^T x_1$ is selected as the Lyapunov function. Next, we directly differentiate V_1 and bring equations (8) and (21) into the equation; we can get

$$\begin{aligned}\dot{V}_1 &= {x_1}^T(t)\dot{x_1}(t) = {x_1}^T(t)x_2(t) \le {x_1}^T(t)(-x_1(t) + s(t))\\ &\le -||x_1(t)||^2 + ||x_1(t)||||s(t)||\\ &\le -||x_1(t)||^2 + \frac{\alpha}{L}||x_1(t)||.\end{aligned} \tag{17}$$

If $||x_1(t)| | > \alpha/L$, then $\dot{V}_1 < 0$ holds, and then this $x_1(t)$ will approach the Ω region. Therefore, this state vector $x_1(t$) is finally bounded and proved.

3.3. Event-Driven Control Strategy. The trigger condition design must ensure the stability of the system. As can be seen from the previous chapter, the relationship (9) is a sufficient condition for the existence of the actual sliding mode. Therefore, this relationship satisfies the stability of the system at any time. In other words, the choice of a driving scheme should make this relationship always hold. Therefore, the trigger scheme is expressed as follows:

$$t_{i+1} = \inf\{t > t_i : L||\mathbf{c}||||\mathbf{e}(t)|| > \sigma\alpha\}. \tag{18}$$

Here, $\sigma \in (0, 1)$. This trigger strategy satisfies the following relationship:

$$L||\mathbf{c}||||\mathbf{e}(t)|| > \sigma\alpha. \tag{19}$$

When $t > 0$, this relationship is always true.

Select $\{t_i\}_{i=0}^{\infty}$ as a trigger sequence. For the stability of the event-driven control system, there must be a positive lower bound between the two trigger intervals, so as to avoid the occurrence of the Zeno phenomenon. In fact, this is a very important process to perform this control task; otherwise, the system may be unstable. In practice, the control law is applied to discrete-time series, and this time series does not

consider the delay caused by control. If this delay is very small and does not affect the performance of the system, then this delay can be ignored. Through this delay-free control execution, we prove that the trigger sequence generated by (18) is the following theorem. Before proving this, we must first write the system dynamics equation (1) in the following format:

$$\dot{\mathbf{x}} = f(\mathbf{x}) + \mathbf{B}u + \mathbf{B}d. \tag{20}$$

$\mathbf{B}=[0, B_2]^T$, where 0 is a column vector with dimension n -1, and all parameters are zero.

Theorem 4. *Considering the above system and the given control law, it can be seen that this trigger sequence is eligible, that is, for the above trigger criteria given by* $\{t_i\}_{i=0}^{\infty}$, *the internal time trigger The interval* T_i *always has a positive lower bound. Here we can give*

$$T_i \geq \frac{1}{L} \ln\left(1 + \sigma \frac{\alpha}{||\boldsymbol{c}||(\rho_N(||\boldsymbol{x}(t_i)||) + \beta_N}\right). \tag{21}$$

In the above formula, β_N *is defined as*

$$\beta_N = \left|\left|\mathbf{B}\mathbf{B}_2^{-I}\right|\right|K + |\mathbf{B}_2|d_0. \tag{22}$$

$\rho_N(||\mathbf{x}(t_i)||)$ *is defined as*

$$\rho_N(||\mathbf{x}(t_i)||) = L\left(1 + \left|\left|\mathbf{B}\mathbf{B}_2^{-1}c^T\right|\right|\right)||\mathbf{x}(t_i)||. \tag{23}$$

Proof. The first thing to be clear is that $\|\mathbf{e}(t)\|$ grows from 0 to $\sigma\alpha/||\mathbf{c}|\,|\,L$; that is, it is bounded. Define the interval $\Gamma =: \{t \in [t_i, t_{i+1}): ||\mathbf{e}(t)|| = 0\}$. Then we can differentiate on $\|\mathbf{e}(t)\|$, and we get

$$\begin{aligned}\frac{d}{dt}\|\mathbf{e}(t)\| &\leq \left\|\frac{d}{dt}\mathbf{e}(t)\right\| = \left\|\frac{d}{dt}\mathbf{x}(t)\right\| \\ &= \|f(\mathbf{x}(t)) + \mathbf{B}u(t) + \mathbf{B}d(t)\| \\ &= \left\|f(\mathbf{x}(t)) - \mathbf{B}\mathbf{B}_2^{-1}c^T f(x(t_i))\right. \\ &\quad \left. - \mathbf{B}\mathbf{B}_2^{-1}K\text{signs}(t_i) + \mathbf{B}d(t)\right\|.\end{aligned} \tag{24}$$

The final equation is obtained by replacing the control expression (5). Using $x(t) = x(t_i) - \mathbf{e}(t)$. We can get further

$$\begin{aligned}\frac{d}{dt}||\mathbf{e}(t)|| \leq L\|\mathbf{x}(t)\| &+ \left\|\mathbf{B}\mathbf{B}_2\left(\mathbf{c}^T\mathbf{B}\right)^{-1}\mathbf{c}^T f(\mathbf{x}(t_i))\right\| \\ &+ \left|\left|\mathbf{B}\mathbf{B}_2^{-1}\right|\right|K + \|\mathbf{B}_2 d(t)\| \leq L(\|\mathbf{x}(t_i)\| \\ &+ \|\mathbf{e}(t)\|) + L\left\|\mathbf{B}\mathbf{B}_2\left(\mathbf{c}^T\mathbf{B}\right)^{-1}\mathbf{c}^T\right\|\|\mathbf{x}(t_i)\| \\ &+ \left|\left|\mathbf{B}\mathbf{B}_2^{-1}\right|\right|K + |\mathbf{B}_2|d_0 = L\|\mathbf{e}(t)\| \\ &+ \left(1 + \left|\left|\mathbf{B}\mathbf{B}_2^{-1}\mathbf{c}^T\right|\right|\right)L\|\mathbf{x}(t_i)\| + \beta_N = L\|\mathbf{e}(t)\| \\ &+ \rho_N(\|\mathbf{x}(t_i)\|) + \beta_N,\end{aligned} \tag{25}$$

where β_N and $\rho_N(\|\boldsymbol{x}(t_i)\|)$ are defined as (22) and (23), respectively. For $t \in [t_i, t_{i+1})$, the solution of the above differential inequality is to call Lemma 2 [38] with the initial condition $\|\boldsymbol{e}(t_i)\| = 0$, and we get

$$||\mathbf{e}(t)|| \leq \frac{\rho_N(||\boldsymbol{x}(t_i)||) + \beta_N}{L}\left(e^{L(t-t_i)} - 1\right). \tag{26}$$

Once (18) is satisfied, time t_{i+1} will be triggered. So we write (26) as

$$\frac{\sigma\alpha}{L||\mathbf{c}||} = ||\mathbf{e}(t_i)|| \leq \frac{\rho_N(||\boldsymbol{x}(t_i)||) + \beta_N}{L}\left(e^{LT_i} - 1\right). \tag{27}$$

Rearrange (27) to get expression (21) for execution time. It still shows that it is bounded by some finite positive number. Note that $\rho(||\mathbf{x}(t_i)||)$ and β_N are both finite positive numbers. Therefore, this means that T_i is proved to be bounded by a positive finite number all the time.

4. Variable Threshold Events Driven by the Sliding Mode Control

4.1. Problem Statement. As can be seen from the previous section, the choice of α determines the steady-state range of the system. Therefore, a large enough value must be selected so that the accumulation performed by the controller does not occur; that is, the driven time is greater than the given minimum time period. For example, for a given small α, the next trigger moment may be lower than the sampling interval corresponding to the processor bandwidth. If this situation happens, the control will not be performed until the trigger time exceeds the processor's bandwidth limit and eventually results in the Zeno phenomenon. In other words, T_i must have a positive lower bound to ensure that this phenomenon does not occur. For all $i \in T_i \geq 0$, we provide the following conditions under the condition of α to ensure that the interactive execution time T_i is greater than the processor bandwidth. A value large enough must be chosen to produce T_i that is greater than the processor's minimum internal execution time τ. However, higher α may increase the steady-state boundary of the sliding trajectory. Therefore, the appropriate optimal value of α is selected to make the system get the best performance under the expected steady-state boundary.

On the other hand, it can be known from Theorems 3 and 4 that the magnitude of the alpha value determines the difficulty of the event-driven and the size of the trigger interval. The larger the alpha value, the more difficult the event trigger occurs and the larger the corresponding event trigger interval. Therefore, under the condition that the above-mentioned system is stable, a larger value of α will reduce the number of events driven and reduce the actuator's frequency of execution. Based on the principle of sliding mode motion, there are two stages of sliding mode motion, as shown in Figure 2: the first stage is moving from the sliding mode surface to the sliding mode surface, and the second is moving on the sliding mode surface and finally reaches the system origin. It is generally known that chattering occurs on the sliding surface. If the current point of motion is far away from the sliding surface, an appropriate increase in K

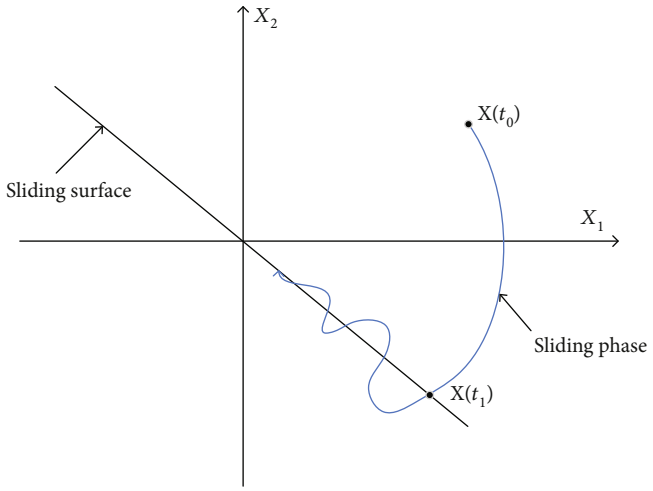

Figure 2: Sliding mode diagram.

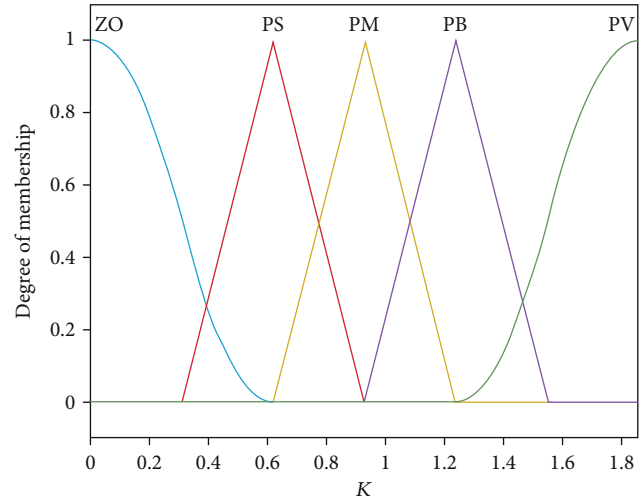

Figure 3: The membership function.

is required to speed up the control and improve the control performance. However, when the distance between the current moving point and the sliding surface is close, in order to reduce the tremor, the approach speed is expected to be reduced, which needs to be reduced by K. Based on the above knowledge and control experience, fuzzy control laws and fuzzy control systems can be designed. K_i may change with the distance between the current moving point and the sliding surface to reduce jitter and system steady-state error.

4.2. Design of Fuzzy Controller. Based on the above ideas, a two-dimensional fuzzy controller is used to directly design the event trigger parameter α and the parameter K of the approach law through the fuzzy control law. It adjusts α and K in real-time according to the absolute value of S and the modulus value of x.

The inputs of the fuzzy controller are set as $\|\mathbf{x}\|$ and $|S|$, which are fuzzification variables of $\mathbf{x}(t)$ and $s(t)$, respectively. The output of the fuzzy controller is the event trigger parameter α and the parameter K of the sliding mode controller blurring variable.

(1) Defining fuzzy sets

$$\begin{aligned} \text{PV} &= \text{positive oversized}, \\ \text{PB} &= \text{positive large}, \\ \text{PM} &= \text{positive middle}, \\ \text{PS} &= \text{positive small}, \\ \text{ZO} &= \text{zero} \end{aligned} \tag{28}$$

(2) According to the fuzzy control principle, $\|\mathbf{x}\|$and $|S|$ are defined as the inputs of the fuzzy controller, and the output of the fuzzy controller is alpha and K

$$\begin{aligned} \|\mathbf{x}\| &= \{\text{ZO, PS, PM, PB, PV}\}, \\ |S| &= \{\text{ZO, PS, PM, PB, PV}\}, \\ \text{Alpha} &= \{\text{ZO, PS, PM, PB, PV}\}, \\ K &= \{\text{ZO, PS, PM, PB, PV}\} \end{aligned} \tag{29}$$

Its field of discussion is as follows:

$$\begin{aligned} \|\mathbf{x}\| &= \{0,+1,+2,+3,+4\}, \\ |S| &= \{0,+1,+2,+3,+4\}, \\ \text{Alpha} &= \{0,+1,+2,+3,+4\}, \\ K &= \{0,+1,+2,+3,+4\} \end{aligned} \tag{30}$$

(3) The membership function setting is shown in Figure 3

(4) Determine the fuzzy control rules of the fuzzy sliding mode controller

According to control experience, when $|S|$ is PB, it means that the state of the system is far from the sliding surface. Therefore, a large approach law parameter is needed to accelerate the approach speed; that is, K should be PB; when $|S|$ is PS, it means that the system state is closer to the sliding mode surface, so a smaller K is required to slow the approach speed to reduce chattering; that is, K should be PS. When $\|\mathbf{x}\|$ is large, it means that the system is far away from the system equilibrium point and has a faster approach speed. The system needs a larger α to reduce the number of triggers. When $\|\mathbf{x}\|$ is small, the system enters near the sliding mold surface, α is not easy to be too large, and it will not trigger if it is too large. Based on the above experience, the control rule table

Table 1: Table of control rules.

Alpha		$\|\|\mathbf{x}\|\|$				
		ZO	PS	PM	PB	PV
$\|S\|$	ZO	ZO	PS	PM	PB	PS
	PS	ZO	PS	PS	PM	PM
	PM	ZO	PS	PM	PB	PB
	PB	ZO	PM	PB	PB	PV
	PV	ZO	PS	PM	PB	PV

Table 2: Table of control rules.

K		$\|\|\mathbf{x}\|\|$				
		ZO	PS	PM	PB	PV
$\|S\|$	ZO	ZO	PS	PM	PB	PS
	PS	ZO	PS	PS	PM	PM
	PM	ZO	PS	PM	PB	PB
	PB	ZO	PM	PB	PB	PV
	PV	ZO	PS	PM	PB	PV

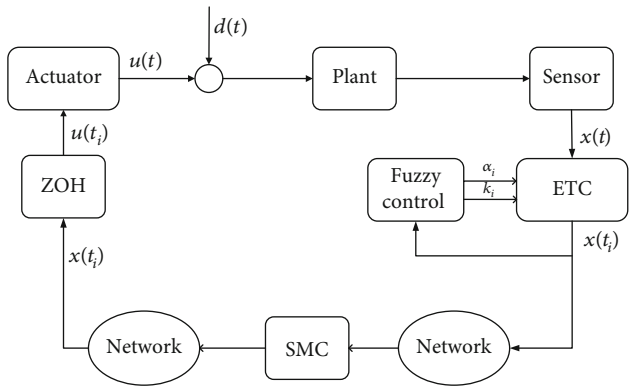

Figure 4: Block diagram of the control system.

shown in Tables 1 and 2 is used. The fuzzy rules used are as follows: if $\|\mathbf{x}\|$ is A and $|S|$ is B, then alpha is C and K is D.

(5) In anti-fuzzy, use the center of gravity method to refine the fuzzy output; the formula is as follows:

$$\varepsilon_0 = \frac{\sum_{i=1}^{n} \mu_{B'}(b_i) \bullet b_i}{\sum_{i=1}^{n} \mu_{B'}(b_i)} \tag{31}$$

The above-mentioned fuzzy controller is used to adjust s in real time, thereby forming a fuzzy reaching law of sliding mode control. The block diagram of the control system is shown in Figure 4.

The law of control is written as follows:

$$u(t) = -\mathbf{B}_2^{-1}\left(\mathbf{c}^T f(x(t_i)) + K_i \operatorname{sign} s(t_i)\right). \tag{32}$$

The trigger scheme is expressed as follows:

$$t_{i+1} = \inf\{t > t_i : L||\mathbf{c}||||\mathbf{e}(t)|| > \sigma\alpha_i\}. \tag{33}$$

Internal time trigger interval T_i is positive lower bound:

$$T_i \geq \frac{1}{L} \ln\left(1 + \sigma \frac{\alpha_i}{||\boldsymbol{c}||(\rho_N(||\boldsymbol{x}(t_i)||) + \beta_N}\right). \tag{34}$$

In the above formula, β_N is defined as

$$\beta_N = \left|\left|\mathbf{B}\mathbf{B}_2^{-1}\right|\right| K_i + |\mathbf{B}_2| d_0. \tag{35}$$

And $\rho_N(||\boldsymbol{x}(t_i)||)$ is defined as follows:

$$\rho_N(\|\mathbf{x}(t_i)\|) = L\left(1 + \left|\left|\mathbf{B}\mathbf{B}_2^{-1}\mathbf{c}^T\right|\right|\right)\|\mathbf{x}(t_i)\|. \tag{36}$$

5. Experimental Simulation

Numerical examples are used in this section to verify the above analysis. Consider the following second-order nonlinear continuous system:

$$\dot{x}_1 = x_2\, \dot{x}_2 = x_1 + x_2^2 + u + d. \tag{37}$$

The compact domain of the system is selected as $D = \{\mathbf{x} \in R^2 : \|\mathbf{x}\|^2 = 9\}$. The Lipschitz constant of the system in this domain D is chosen as $L = 10$. The perturbation is assumed to be bounded, and it is considered here as $d = 0.5 \cos t$, which results in $\triangle_d = 0.5$. The design of the sliding surface should ensure the stability of the system. We choose $\mathbf{c}^T = [0.5\ 1]$, so $\mathbf{s} = \mathbf{c}^T\mathbf{x}$ represents the sliding variable in the continuous-time setting. The SMC for (3) can be expressed as follows:

$$u = x_1 - 0.5x_2 - x_2^2 - \mathrm{Ksign}(s). \tag{38}$$

And $K > 0.5$. When the control law is implemented through an event-driven strategy, it remains constant in the time interval $[t, t_{i+1})$, that is, at $t \in [t_i, t_{i+1})$, $u(t) = u(t_i)$, and $i \in Z \geq 0$. The other parameters are chosen as $\tau^* = 0.0001$ and $\sigma = 0.8$. The initial value of $\alpha_{\min}$ is chosen to be 0.3. The initial value is $K = 0.8$, and the sampling period is set to $ts = 0.001$ s. The initial conditions is [-1 2].

Case 1. EDSM.

Figure 5 shows the simulation results of the response of EDSM to a nonlinear system.

It can be seen from Figure 5(a) that the actual sliding pattern occurs in the system in a limited time. For the selected value of a, the value of the sliding mode band is 0.03. The sliding trajectory entered the frequency band for a limited time and remained there. The same is true for different perturbation range values. The change of the state trajectory over time is shown in Figure 5(b), which shows that the trajectory is finally in a stable state, so the system is in a stable state. The interevent time versus time is shown in Figure 5(d). After entering the sliding mode, the driving time

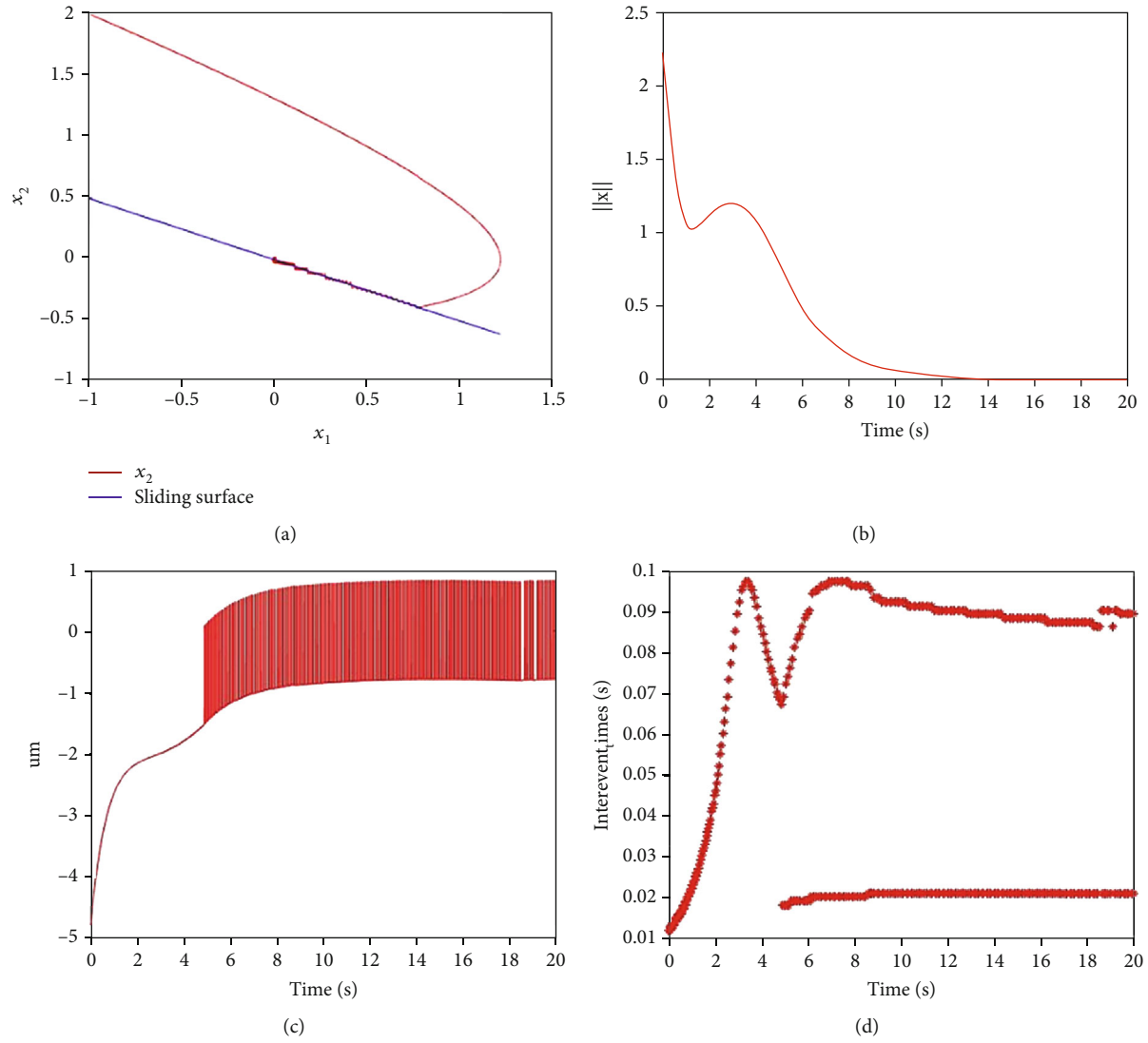

Figure 5: EDSMC system response diagram. (a) System trajectory diagram showing the actual sliding mode in a limited time. (b) System status. (c) Sliding mode control with event touch. (d) Mutual execution time of event-driven sliding mode control.

interval has a sequence of long and short. The controller output control signal is updated as shown in Figure 5(c). After entering the sliding mode, it is in a continuous oscillation state.

Case 2. AEDSM.

Figures 6–8 show the simulation results of AEDSM response to a nonlinear system.

It can be seen from Figure 6 that, as in the above case, the sliding track enters the frequency band in a limited time. For the selected α value, due to the variable adjustment of the K value, the sliding mode band is reduced to 0.02 compared to the above case. The same is true for different perturbation range values. The trajectory is finally in a stable state. The above illustrates the effectiveness of the proposed variable event-driven transmission strategy.

It can be seen from Figure 7 that α of AEDSMC is continuously adjusted and its corresponding threshold is continuously adjusted until the error reaches a steady state. In this case, α eventually converged to 0.2039. In this case, K eventually converged to a constant value.

Figure 8 shows the change in the S-function modulus. It can be seen that the S-function modulus is most stable in the sliding mode band, which is 0.02.

Compared with the EDSMC control scheme, the AEDSMC sliding mode band is 30% smaller than the above situation, effectively suppressing the sliding mode chattering phenomenon. The proposed driving scheme has a smaller number of driving events and a longer event driving interval, so it has better performance in terms of limited resource utilization. Table 3 summarizes the results and shows the number of trigger events.

6. Summary

In this paper, a variable threshold control method based on event driving was proposed and designed to solve the

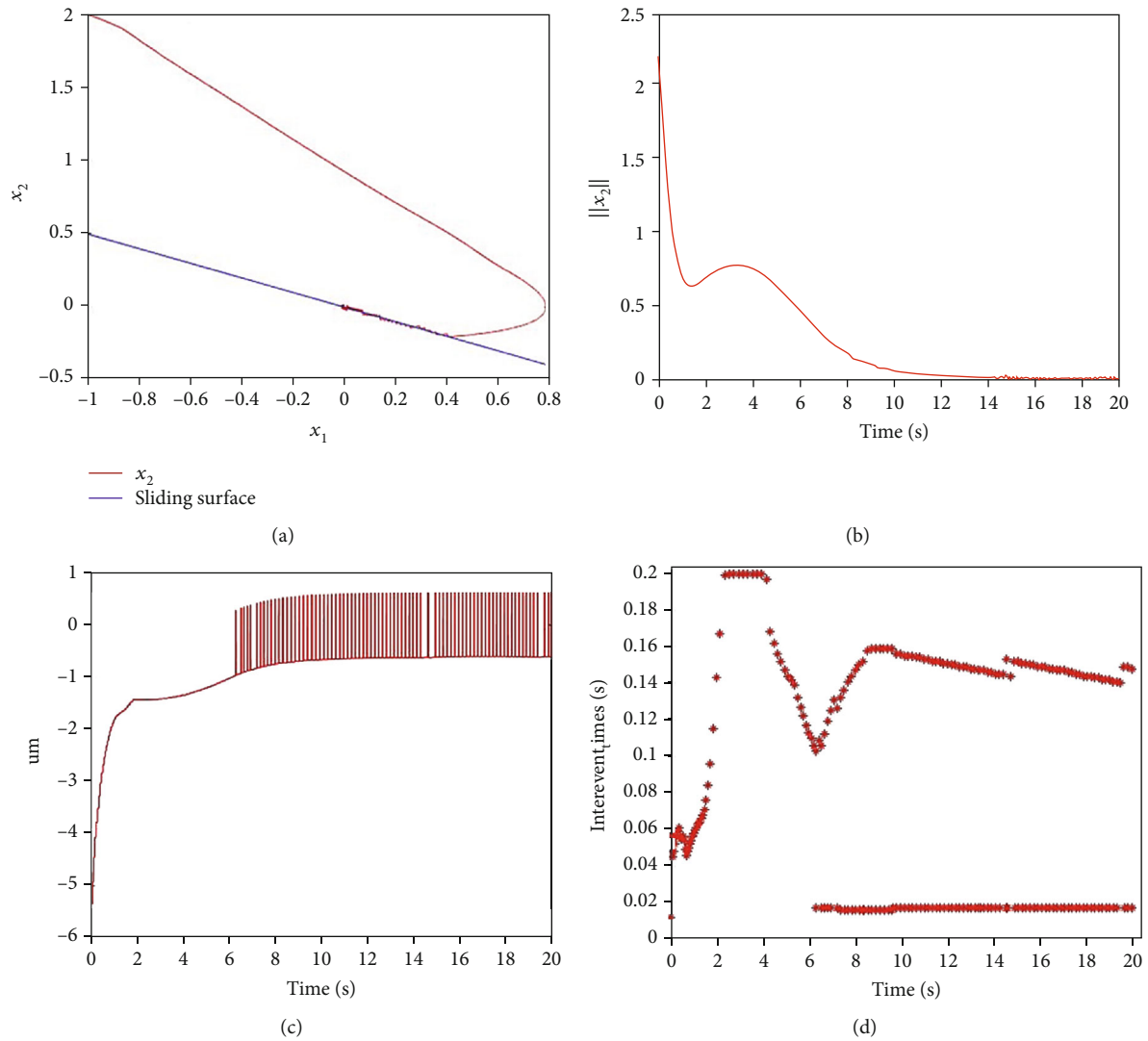

Figure 6: AEDSMC system response diagram. (a) System trajectory diagram showing the actual sliding mode in a limited time. (b) System status (c) Sliding mode control with event touch. (d) Mutual execution time of event-driven sliding mode control.

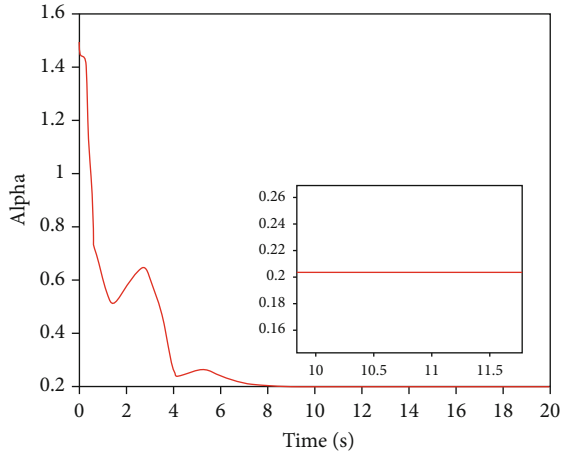

Figure 7: Variable parameter α adjustment.

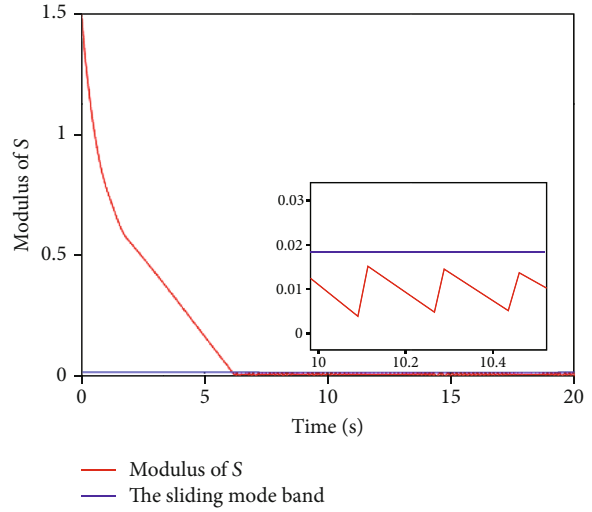

Figure 8: S-mode modulus change.

Table 3: Comparison of results.

	SMC	EDSMC	AEDSMC
Total number of triggers	20000	410	226
Stability error of 20 s	0	0.014	0.010
Sliding manifold	0.025	0.03	0.02
Min trigger event interval	0.001	0.012	0.016
Max trigger event interval	0.001	0.097	0.2

problem of insufficient robustness of a class of nonlinear network systems with external disturbances. Different from the current event-driven control system, the control scheme proposed in this paper can variably update the threshold parameter α according to the fuzzy rule after each event is driven and simultaneously update the parameter K of the sliding mode controller. In this scheme, the system with external disturbance has good robustness and adaptability. Simulation results show that the event-driven control scheme reduces the number of event triggers, saves system network resources, effectively suppresses the chattering phenomenon of sliding mode control, and meets system design performance requirements, which verifies the effectiveness and feasibility of the scheme. In the future work, we can consider other interferences, such as denial-of-service (DOS) attacks and study adaptive event-driven control in network control systems under DOS attacks.

Data Availability

The specific data description has been mentioned in detail in the paper.

Conflicts of Interest

The authors declare that they have no conflicts of interest.

Acknowledgments

This work was supported by the Key Fund of Shaanxi Province Natural Science Basic Research Program (2019JLZ-06) and Key Project of National Internet of Things Integrated Innovation and Integration (2018-470).

References

[1] D. Zhang, P. Shi, Q.-G. Wang, and L. Yu, "Analysis and synthesis of networked control systems: a survey of recent advances and challenges," *ISA Transactions*, vol. 66, pp. 376–392, 2017.

[2] X. Ge, Q.-L. Han, D. Ding, X.-M. Zhang, and B. Ning, "A survey on recent advances in distributed sampled-data cooperative control of multi-agent systems," *Neurocomputing*, vol. 275, pp. 1684–1701, 2018.

[3] X. Jia, D. Zhang, X. Hao, and N. Zheng, "Fuzzy H(infinity) tracking control for nonlinear networked control systems in T-S fuzzy model," *IEEE Transactions on Systems, Man and Cybernetics, Part B: Cybernetics*, vol. 39, no. 4, pp. 1073–1079, 2009.

[4] F. Yang and Q.-L. Han, "_H_ $_\infty$ control for networked systems with multiple packet dropouts," *Information Sciences*, vol. 252, pp. 106–117, 2013.

[5] C. Peng, Q.-L. Han, and D. Yue, "Communication-delay-distribution-dependent decentralized control for large-scale systems with ip-based communication networks," *IEEE Transactions on Control Systems Technology*, vol. 21, no. 3, pp. 820–830, 2013.

[6] W. Chen and L. Qiu, "Stabilization of networked control systems with multirate sampling," *Automatica*, vol. 49, no. 6, pp. 1528–1537, 2013.

[7] P. Ogren, E. Fiorelli, and N. E. Leonard, "Cooperative control of mobile sensor networks: adaptive gradient climbing in a distributed environment," *IEEE Transactions on Automatic Control*, vol. 49, no. 8, pp. 1292–1302, 2004.

[8] N. H. Gartner, C. Stamatiadis, and P. J. Tarnoff, "Development of advanced traffic signal control strategies for intelligent transportation systems: multilevel design," *Transportation Research Record*, vol. 1494, pp. 98–105, 1995.

[9] C. Meng, T. Wang, W. Chou, S. Luan, Y. Zhang, and Z. Tian, "Remote Surgery Case: Robot-Assisted Teleneurosurgery," in *Proceedings of the 2004 IEEE Conference on Robotics and Automation ICRA04)*, pp. 819–823, New Orleans, USA, 2004.

[10] T. C. Yang, "Networked control system: a brief survey," *IEE Proceedings-Control Theory and Applications*, vol. 153, no. 4, pp. 403–412, 2006.

[11] G. Buttazzo and A. Cervin, "Comparative assessment and evaluation of jitter control methods," in *Proceedings of the 15th conference on Real-Time and Network Systems*, pp. 163–172, Nancy, France, March 2007.

[12] R. Luck and A. Ray, "An observer-based compensator for distributed delays," *Automatica*, vol. 26, no. 5, pp. 903–908, 1990.

[13] C. Tan, L. Li, and H. Zhang, "Stabilization of networked control systems with both network-induced delay and packet dropout," *Automatica*, vol. 59, pp. 194–199, 2015.

[14] R. Luck and A. Ray, "An observer-based compensator for distributed delays," *Automatica*, vol. 26, no. 5, pp. 903–908, 2003.

[15] J. Nilsson and B. Bernhardsson, "Analysis of real-time control systems with time delays," in *Proceedings of the 35th IEEE Conference on Decision and Control*, vol. 3, pp. 3173–3178, Kobe, Japan, 1996.

[16] G. P. Liu, Y. Xia, J. Chen, D. Rees, and W. Hu, "Networked predictive control of systems with random network delays in both forward and feedback channels," *IEEE Transactions on Industrial Electronics*, vol. 54, no. 3, pp. 1282–1297, 2007.

[17] K. J. Aström, "Event based control," in *Analysis and Design of Nonlinear Control Systems*, pp. 127–147, Springer, Berlin, 2008.

[18] W. Heemels, J. Sandee, and P. Van Den Bosch, "Analysis of event-driven controllers for linear systems," *International Journal of Control*, vol. 81, no. 4, pp. 571–590, 2008.

[19] W. Heemels, K. H. Johansson, and P. Tabuada, "An introduction to event-triggered and selftriggered control," in *2012 IEEE 51st Annual Conference on Decision and Control (CDC)*, pp. 3270–3285, Hawaii, December 2012.

[20] Y. Ke-You and X. Li-Hua, "Survey of recent progress in networked control systems," *Acta Automatica Sinica*, vol. 39, no. 2, pp. 101–117, 2013.

[21] H. Yu and P. J. Antsaklis, "Event-triggered output feedback control for networked control systems using passivity:

achieving stability in the presence of communication delays and signal quantization," *Automatica*, vol. 49, no. 1, pp. 30–38, 2013.

[22] P. Tabuada, "Event-triggered real-time scheduling of stabilizing control tasks," *IEEE Transactions on Automatic Control*, vol. 52, no. 9, pp. 1680–1685, 2007.

[23] P. Tallapragada and N. Chopra, "Decentralized event-triggering for control of nonlinear systems," *IEEE Transactions on Automatic Control*, vol. 59, no. 12, pp. 3312–3324, 2014.

[24] W. Heemels and M. C. F. Donkers, "Model-based periodic event-triggered control for linear systems," *Automatica*, vol. 49, no. 3, pp. 698–711, 2013.

[25] E. Tian, D. Yue, and C. Peng, "Quantized output feedback control for networked control systems," *Information Sciences*, vol. 178, no. 12, pp. 2734–2749, 2008.

[26] W.-W. Che, J.-L. Wang, and G.-H. Yang, "Quantised H^{∞} filtering for networked systems with random sensor packet losses," *IET Control Theory & Applications*, vol. 4, no. 8, pp. 1339–1352, 2010.

[27] M. Mazo and P. Tabuada, "Decentralized event-triggered control over wireless sensor/actuator networks," *IEEE Transactions on Automatic Control*, vol. 56, no. 10, pp. 2456–2461, 2011.

[28] X. Wang and M. D. Lemmon, "Event-triggering in distributed networked systems with data dropouts and delays," in *Hybrid systems: computation and control, international conference, HSCC 2009*, pp. 366–380, San Francisco, Ca, USA, April 2009.

[29] F. Forni, S. Galeani, D. Nesic, and L. Zaccarian, "Event-triggered transmission for linear control over communication channels," *Automatica*, vol. 50, no. 2, pp. 490–498, 2014.

[30] A. Seuret, C. Prieur, and N. Marchand, "Stability of non-linear systems by means of event-triggered sampling algorithms," *IMA Journal of Mathematical Control and Information*, vol. 31, pp. 415–433, 2013.

[31] D. Yue, E. Tian, and Q.-L. Han, "A delay system method for designing event-triggered controllers of networked control systems," *IEEE Transactions on Automatic Control*, vol. 58, no. 2, pp. 475–481, 2013.

[32] S. Hu and D. Yue, "Event-triggered control design of linear networked systems with quantizations," *ISA Transactions*, vol. 51, no. 1, pp. 153–162, 2012.

[33] C. Peng, Q.-L. Han, and D. Yue, "To transmit or not to transmit: a discrete event-triggered communication scheme for networked Takagi-Sugeno fuzzy systems," *IEEE Transactions on Fuzzy Systems*, vol. 21, no. 1, pp. 164–170, 2013.

[34] S. Hu and D. Yue, "L2-Gain analysis of event-triggered networked control systems: a discontinuous Lyapunov functional approach," *International Journal of Robust and Nonlinear Control*, vol. 23, no. 11, pp. 1277–1300, 2013.

[35] V. I. Utkin, *Sliding Modes in Control and Optimization*, Springer-Verlag, 1992.

[36] S. K. S. Christopher Edwards, *Sliding Mode Control*, Taylor and Francis, 1998.

[37] X. H. Liu, X. H. Yu, G. Q. Ma, and H. S. Xia, "On sliding mode control for networked control systems with semi-Markovian switching and random sensor delays," *Information Sciences*, vol. 337, pp. 44–58, 2016.

[38] H. Khalil, *Nonlinear Systems*, NJ: Prentice-Hall, Upper Saddle River, 3rd edition, 2002.